Chapter 2. Air-cooled Air Gap Membrane Distillation Module

2.1. Introduction

Experimental setups, the AGMD module and superhydrophobic surface preparation are described in this chapter. Further in this chapter, the results from the different configurations have been discussed followed by the conclusions that can be inferred from these results. The validation of results is followed by the parametric study in which the effect of the various parameters on the performance of the process is studied.

2.2 Experimental setup and the AGMD module

The schematic of the experimental setup to perform various optimization and parametric studies on considered AGMD module is shown in Figure 1. The feed water is stored in 5 gallon tank and an immersion water heater with a thermostat is used to keep the feed water at a temperature which is within ± 0.2 ^{0}C of the desired temperature. The feed water is pumped to the AGMD module by a revolution water pump (12 VDC, 7.5 Amps). It had a maximum flow rate of 3 GPM and the shutoff pressure of 3.8 bars. A flowmeter was used to measure the flow rate of the feed water. Thermocouples were used to monitor the water temperature at the inlet and outlet and the condensing plate temperature. Instead of using a channel behind the condensing plate, a fan (5 VDC, 0.5 Amps) was placed on the other side of the condensing plate and forced convection was used for cooling purposes.

The effect of membrane material, pore size, thickness, porosity and membrane support on permeate flux for an AGMD process has been studied [54,55]. Bigger pore size, lesser thickness and absence of support structure results in increase in permeate flux. But lack of support structure can result in a fragile membrane which will need to be replaced often. Also, the pore size cannot be very large as it will let impurities through the pores. These considerations led us to choose a polytetrafluoroethylene (PTFE) membrane with propylene support structure, a pore size of 0.45 μm and thickness, t of 160 μm to 230 μm for our experimental module. The membranes for the experiments were supplied by Membrane Solutions, Shanghai, China. The membrane in the module was held in place using an acrylic piece and a mesh. Copper, Aluminum, Steel and Plastic meshes were used for this purpose to study the effect of conductivity oh the support mesh on permeate flux. The AGMD module which was used in the experiments was made from

acrylic. The module contains a saline channel, an air gap and an air-cooled condensing surface. The feed channel is 65 mm X 63 mm X 12.7 mm. The channel is serpentine and has six walls with width 5 mm each to guide the saline feed through the channel. The serpentine channel helps to maximize the time for which the feed comes in contact with the membrane and the pressure on the saline side of the membrane. Alsaadi et al. [54] has shown that the saline residence time inside the AGMD module has a positive effect on the flux.

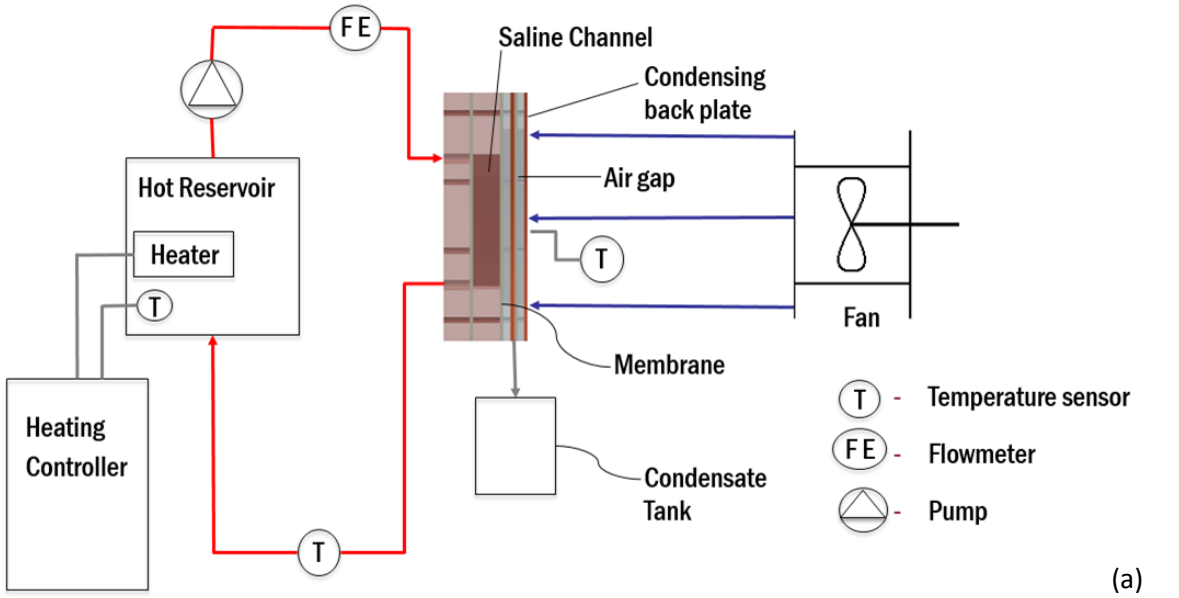

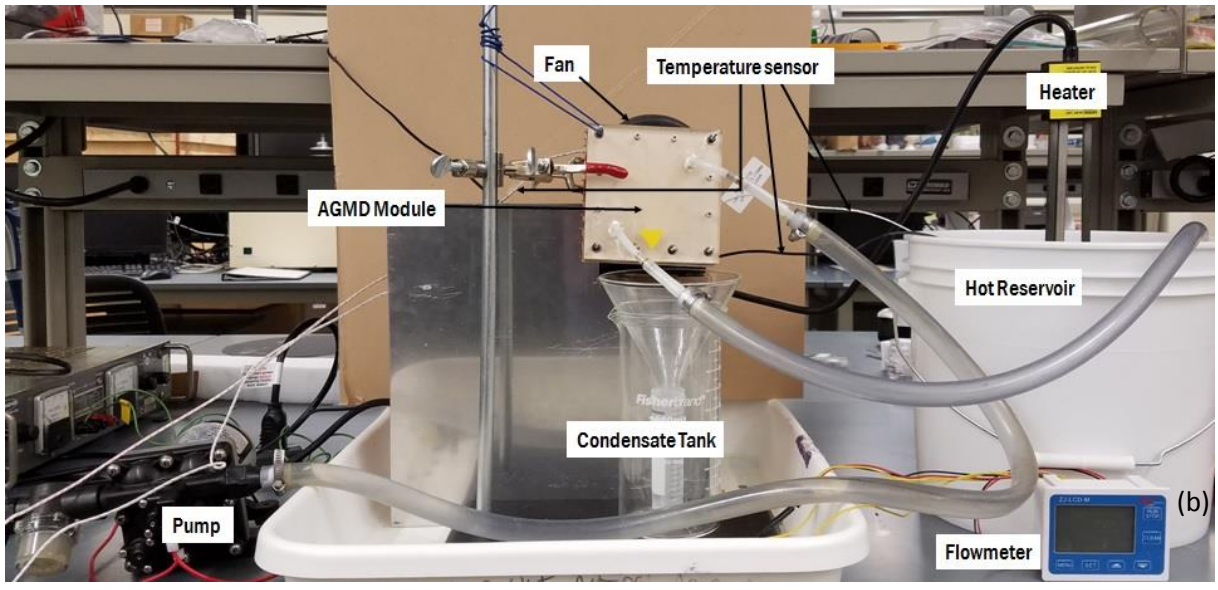

Figure 1. (a) Schematic illustration of the AGMD apparatus diagram for the experiments and the parametric study; and (b) photograph of the setup.

Copper plates were used as condensing surfaces. The vapor which passed through the membrane upon condensing on the back plate was allowed to drip down under the effect of gravity and collected in a flask. The air gap was created by inserting combination of acrylic sheets and gaskets of different thicknesses between the membrane and the condensing plate. When the saline feed water exits the module, its temperature is recorded and it is released back into the feed water storage tank. The ppm level of impurities in the feed water was kept in a range of 150 – 170 ppm by adding water.

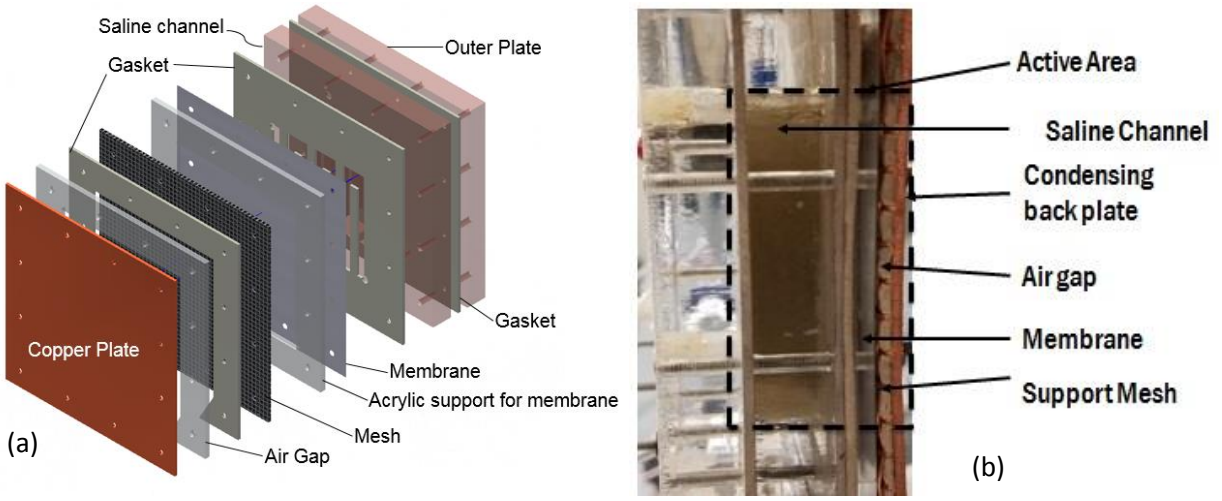

Figure 2. (a)Exploded CAD drawing, (b) photograph of the AGMD air-cooled module used in the experiments.

The effects of various parameters and conditions on the performance of an air-cooled air gap membrane distillation module were studied in this experimental study. The Feed water temperature was varied from 40 to 70 ^{0}C and its effect on the permeate flux was studied. Flow rate of about 2 L/min was maintained by controlling the current input to the circulation pump. The volume of the distillate collected in the flask (V) was measured for a given time (t) to calculate the permeate flux. The effective area of the membrane (A) was also used in this calculation.

$$Flux = \frac{V}{At} \qquad (1)$$

The system was made in form of modules which could be placed in series configuration. This resulted in a scalable design in which the output could be increased or decreased by adding or

removing modules. Effect of hydrophobicity of the copper condensing surface and the hydrophobicity and conductivity of the support mesh were also studied during the trials.

2.3 Superhydrophobic surface preparation and contact angle measurement

In recent times, there have been attempts to develop Graphene based hydrophobic coatings [56-59]. In this study, we have focused on using copper based coatings on the condensing plate. Copper based superhydrophobic surfaces as considered in this study were prepared through an electrodeposition based process to generate inherent and durable superhydrophobic coatings as described by Jain and Pitchumani [60]. Electrodes, copper sheet/mesh and platinum mesh were cleaned with acetone and deionized water to remove any dirt and grease from the surface and employed as working electrode and anode, respectively. Two step electrodeposition process as described by Haghdoost and Pitchumani [61], where application of high potential is followed by a small potential to obtain a multiscale and stable deposit, was employed. The electrolyte was an aqueous solution containing $CuSO_4$ (1 M) and H_2SO_4 (0.5 M). Potentistatic electrodeposition at 1.1 V, followed by electrodeposition at 0.15 V for 10 secs, was performed and inherent copper based deposit was obtained on considered copper back plate and copper mesh. Furthermore, deposition time was optimized to obtain the deposit thickness of about 30μm on the considered sample. After electrodeposition, surfaces were rinsed with acetone and deionized water and dried with nitrogen gas.

As a final step, the as-prepared surfaces were modified through immersion in 0.02 M methanol solution of stearic acid at room temperature for 24 hours. The modified samples were then washed with methanol to remove any residual organic acid on the surface, followed by washing with deionized water and then dried for further characterization and study.

Multiscale cauliflower-shaped morphology was obtained on the prepared superhydrophobic surface, as observed in Fig. 3. Fig. 3 also shows the equivalent drop shape and water contact angle on the prepared superhydrophobic coatings surface. An aggressive fractal texturing with globular asperities at multiple scales leads to the observed superhydrophobicity with contact angles of 159° for the prepared superhydrophobic copper back condensing plate. Presence of multiscale asperities and superhydrophobic nature of the coating ensured the high nucleation density and dropwise and jumping droplet condensation on the superhydrophobic condensing back plate.

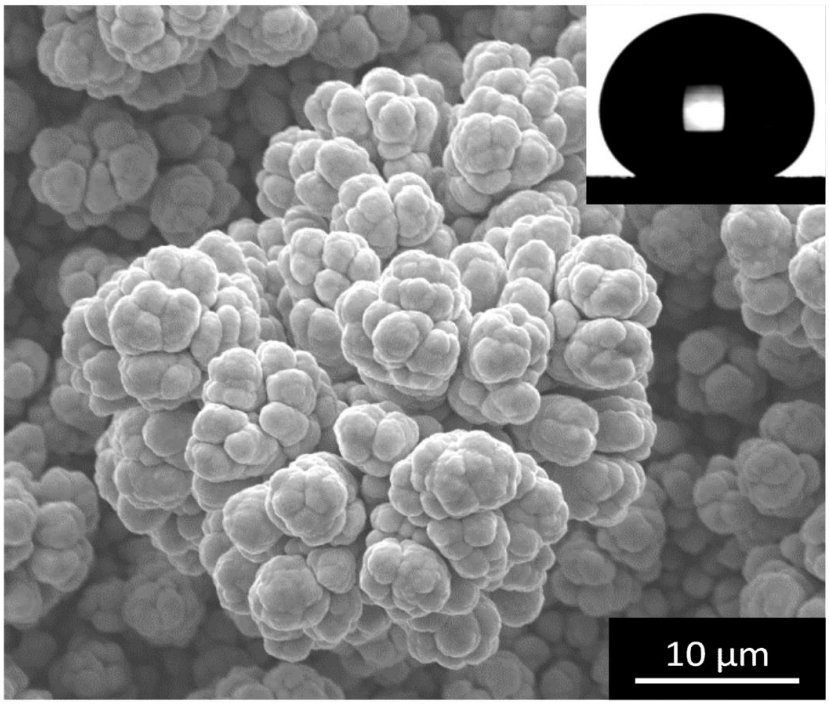

Figure 3. The prepared superhydrophobic surface along with the equivalent drop shape and water contact angle on the prepared superhydrophobic coatings surface

2.4. Results and Discussion

2.4.1 Validation of results

The design and performance of the basic air-cooled AGMD module was validated against previously studied conventional AGMD system design by Warsinger et al [25]. Flux output was compared for a basic AGMD configuration with a plastic mesh as a membrane support and pure copper condensing surface as a back plate. The inconsistencies between presented and previously studied designs such as use of air cooling instead of conventional water cooling channel and different air gap thicknesses, did not allow a straightforward comparison of flux output between two designs. Furthermore, with an increase in saline feed temperature, condensing plate temperature increases, which leads to an improved convective heat transfer from condensing plate to ambient air. Hence, it was not feasible to get a consistent temperature difference between hot saline feed liquid and condensing back plate for the studied configuration at various saline feed temperatures, unlike a conventional water-cooled systems where a constant temperature difference can be maintained for various inlet saline feed temperatures.

To normalize the effect of inconsistencies and allow the validation of designed AGMD configuration, a corrected flux value is specified and considered. Corrected flux approximately modifies the actual flux values to obtain the flux for any different air gap thickness and temperature difference, assuming a linear effect of these parameters and can be given as:

$$\text{Corrected Flux} = \text{Real FLux} * \frac{d}{d_{[25]}} * \frac{\Delta T_{[25]}}{\Delta T} \qquad (2)$$

where, d = air gap [mm]

$d_{[25]}$ = air gap [mm] used by Warsinger et al [25]

ΔT = Temperature difference between the condensing surface and the saline channel

$\Delta T_{[25]}$ = Temperature difference between the condensing surface and the saline channel as reported by Warsinger et al [25]

Real flux and corrected flux values as obtained from the present study for various feed temperatures are compared with the flux output for the conventional AGMD setup described by Warsinger et al [25] and are shown in Figure 4. A similar trend of real flux values between both the studies can be observed from the same. In addition, a small variation of about 5-10% between corrected flux for present study and flux output as reported by Warsinger et al, validates the designed setup and various design and performance parameters. Based on this validation, the air-cooled AGMD system has been optimized through various experimental parametric studies as described in following subsections.

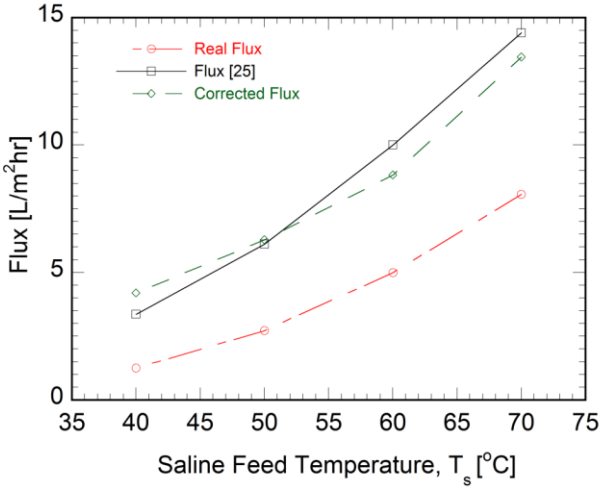

Figure 4. Comparison of the results for the air-cooled AGMD module with the conventional AGMD module results in Warsinger et al [25].

2.4.2 Effect of air gap

A parametric study to study the effect of various system and process variables on the performance of the air-cooled module was conducted. Figure 5 shows the effect of air gap dimensions on the flux for the process. Flux is the parameter which has been used to gauge the performance of the membrane distillation process. The unit for flux is L/m^2hr, where the amount of condensate formed is measured in liters and the area of the membrane exposed for the droplets to cross over is measured in m^2. As can be seen from Figure 5, flux increases somewhat linearly with increase in saline feed temperature. The flux values are highest for the case when the air gap is smallest and it becomes noticeably lower when the air gap increases. It has been shown that an increase in air gap results in decrease in mass flux due to an additional resistance to mass transfer [62].

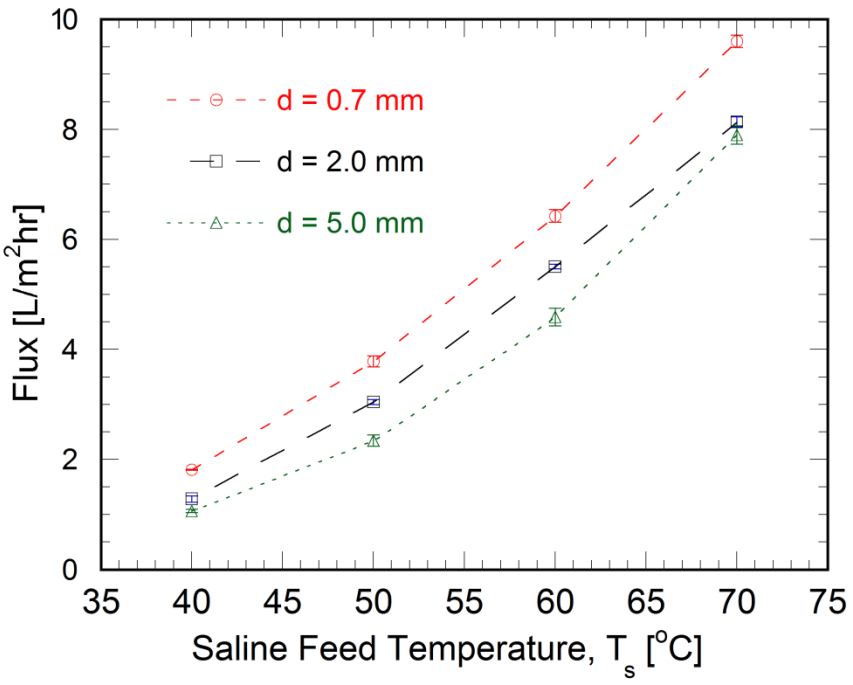

Figure 5. Flux versus Saline Feed Temperature at different air gap, d.

2.4.3 Effect of support mesh conductivity

The effect of mesh conductivity on the flux was studied using Plastic, Steel, Aluminum and Copper meshes. The meshes are essential for holding the membrane in place and reduce bulging of the membrane due to the pressure difference on the two sides. The meshes had an open area in the range of 65% to 66%, so that they do not interfere with the vapor transfer across the

membrane. As can be seen from Figure 6, the module with the Copper mesh performs the best and the plastic mesh results in the lowest yields. The steel and aluminum mesh have flux values between copper and plastic.

It is seen that the modules with meshes that have higher conductivity have higher yields. This is due to better heat conduction across the air gap [25-28]. The highly conductive mesh surfaces reduce resistance to heat transfer in the air gap. When the saline feed temperature is above 60 °C, the air gap in the module gets flooded and the effect of the mesh conductivity is more pronounced at these temperatures.

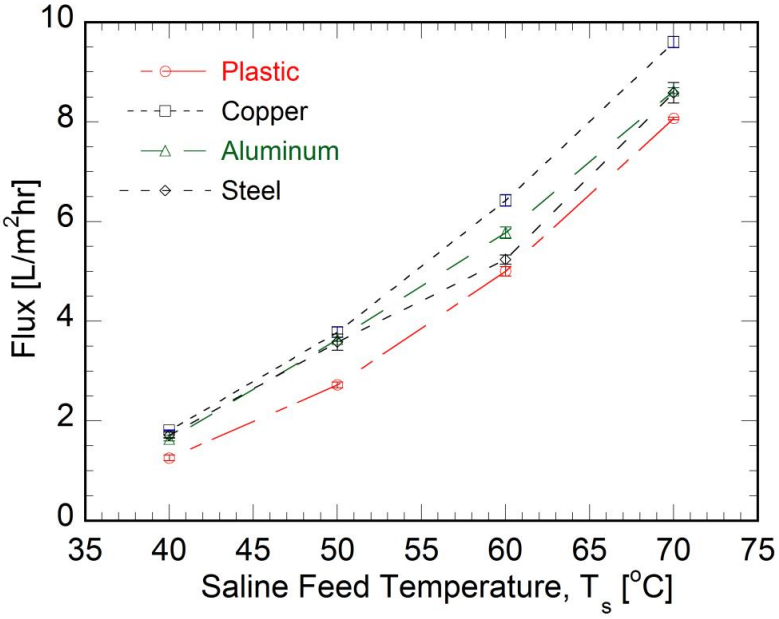

Figure 6. The effect of support mesh with different thermal conductivities on the flux

2.4.4 Effect of hydrophobicity of support mesh and condensing surface with small air gap

Hydrophobic condensing plate and hydrophobic mesh surface also affect the yields for the process. Figure 7 shows the flux values for the different condensing plate and mesh combinations for a small air gap (0.7 mm) configuration. When a control mesh is used which is a normal copper mesh, the modules with hydrophobic back plate have better flux values at lower temperature. This has been attributed to hydrophobic jumping droplet condensation [25-28].

At temperatures above 60 °C, the module with the control back plate surface performs better. This is due to the fact that at these temperatures, the air gap is flooded and both the control surface and the hydrophobic surface behave similarly. The hydrophobic surface has lower yields

at high temperatures because of the fact that thermal conductivity of the condensing plate reduces due to the hydrophobic coating, which results in higher temperature for the back plate and this leads to a lower ΔT which in turn leads to lower yields.

The hydrophobicity of the mesh has a negative effect on the yield which can be seen in Figure 7, this is due to the fact that the mesh is not a condensing surface. The hydrophobic mesh has lower conductivity when compared to control copper mesh and this leads to the lesser yield.

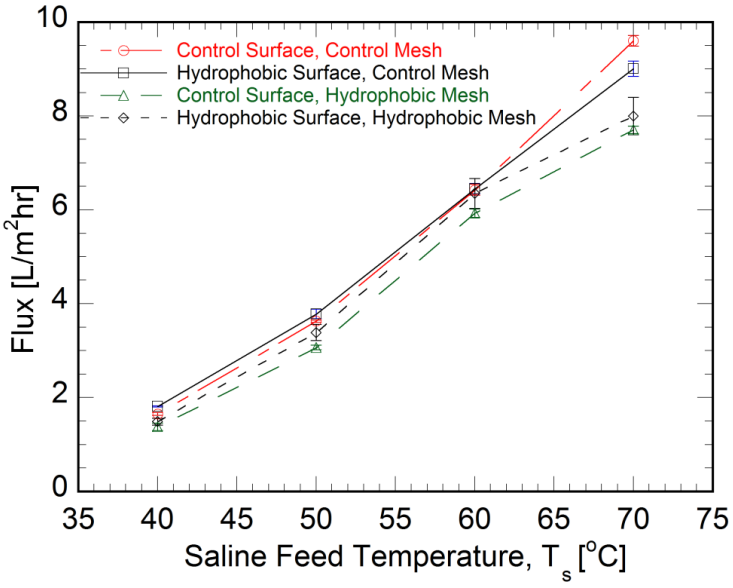

Figure 7. Effect of hydrophobicity of the support mesh and the condensing surface on the flux when air gap, d = 0.7 mm.

2.4.5 Effect of hydrophobicity of support mesh and condensing surface with larger air gap

When the air gap is increased from 0.7 mm to 5.0 mm, the hydrophobic condensing surface performs better than the control surface, as can be seen in Figure 8a. The yield from the module with the control surface improves considerably when the temperature goes beyond 60 °C. Flooding at high temperatures negates the positive effects of hydrophobicity like jumping droplet condensation while the lower conductivity of the hydrophobic surface affects the yield negatively. The hydrophobic mesh surfaces have the same effect as they had in the case of lesser air gap.

The results here show that the conductivity of the mesh, the air gap and the hydrophobicity of the condensing plate have a significant effect on the flux values for the system. The hydrophobicity of the mesh has no significant positive effect on the yield. Figure 8b shows the

effects of both air gap and hydrophobicity of the condensing surface on the yield. From the figure, it can be seen that even though the hydrophobic surface performs better than the control surface at large air gap, the yield it provides is lower than the yield of the control surface module at lesser air gap.

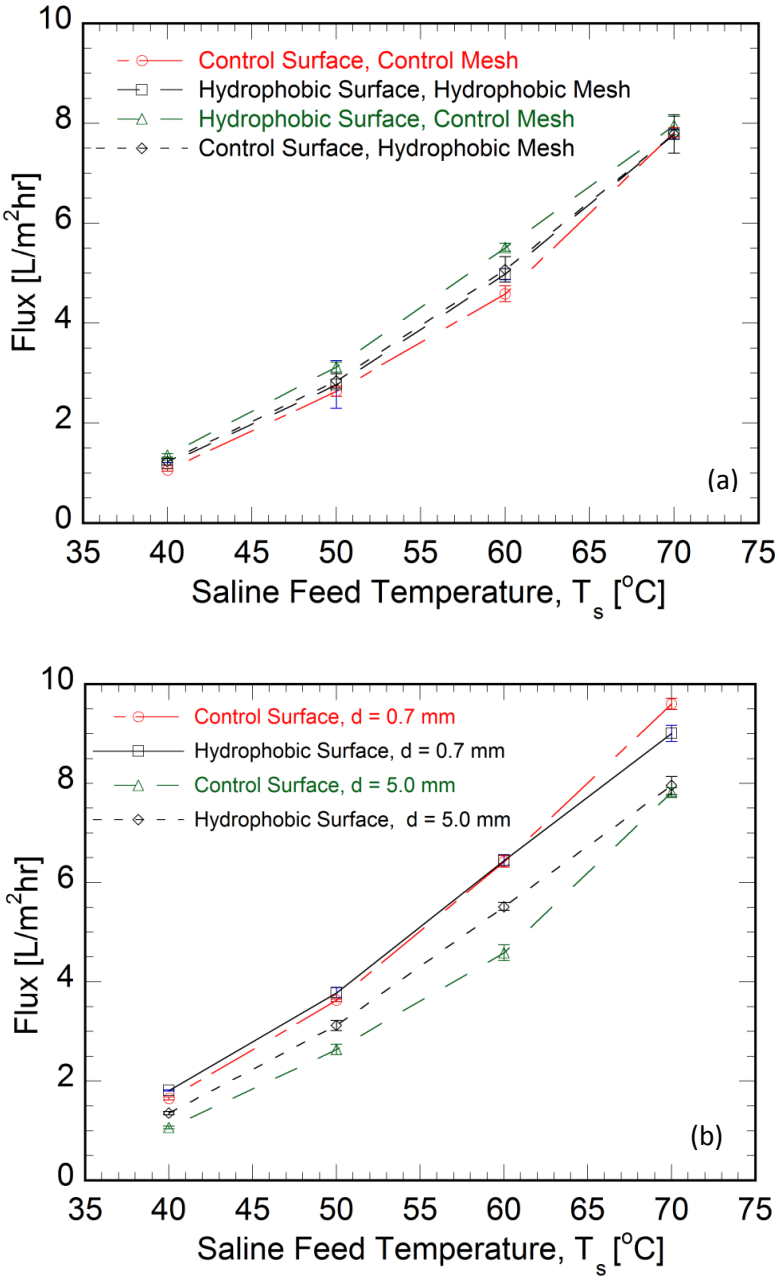

Figure 8. (a) Effect of hydrophobicity of the support mesh and the condensing surface on the flux when air gap, d = 5.0 mm (b) Cumulative effect of the hydrophobicity of the condensing surface and air gap, d on the flux

2.4.6 Effect of air gap and hydrophobicity of the mesh on the saline feed temperature and the cumulative yield in series configuration

Although, the yield from the control surface and small air gap configuration is highest at high temperature (70 °C), using a hydrophobic surface has its own advantages even at such high temperatures, even though the flux is slightly lower. Because of the lower conductivity of the hydrophobic back plate, the temperature drop for the saline water after it passes through the module is less when compared to the control back plate case. This can be useful as lower drop in temperature will lead to lesser heating requirement when it goes to the hot reservoir, which can lead to lesser energy requirements.

The lower drop in saline temperatures can also be useful when the modules are placed in series and the saline coming out of one module is the saline feed for the next module. It can be seen that in such a series configuration, the temperature drop is more in the case of control surface and small air gaps. Large air gap cases have a smaller drop in the saline feed temperature for the consecutive modules.

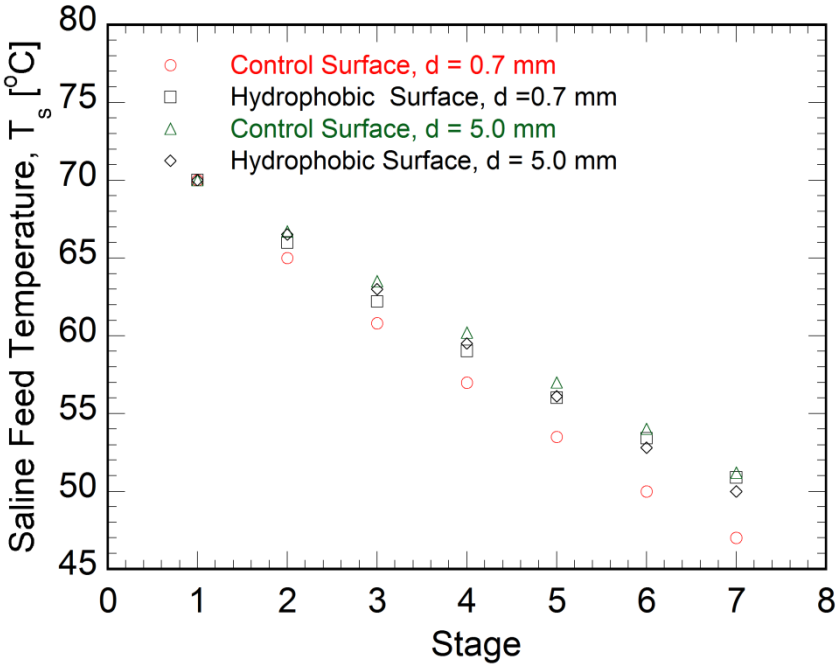

Figure 9. Saline Feed Temperature versus the respective stages during the series configuration trials and the effect of hydrophobicity of the condensing plate and the air gap, d on the same

To study how the different configurations work in a series configuration, the exit saline temperature of the first module was used as the feed saline temperature for the second module and so on. The trials were conducted till the saline feed temperature dropped to below 50 °C, as the flux reduces considerably after that. Figure 9 shows the saline feed temperature for the respective stages. As can be seen from the figure, the feed temperature decreases faster for the control back plate and small air gaps. The corresponding cumulative yields can be seen in Figure 10. The cumulative yield increases sharply for the two configurations with small air gap but as the number of stages increase, the flux readings for hydrophobic surface back plate configuration surges ahead, as it has higher yield for later stages because the temperature drop is less for consecutive stages in this case and lower temperature drop means higher saline feed temperature for a given stage. The saline feed temperature directly affects the flux and thus, it results in higher cumulative flux for hydrophobic surfaces. The highest cumulative flux is generated for the case with hydrophobic condensing plate and small air gap of 0.7 mm. Even the hydrophobic condensing surface with large air gap of 5.0 mm case has better cumulative flux values than the control condensing surface cases.

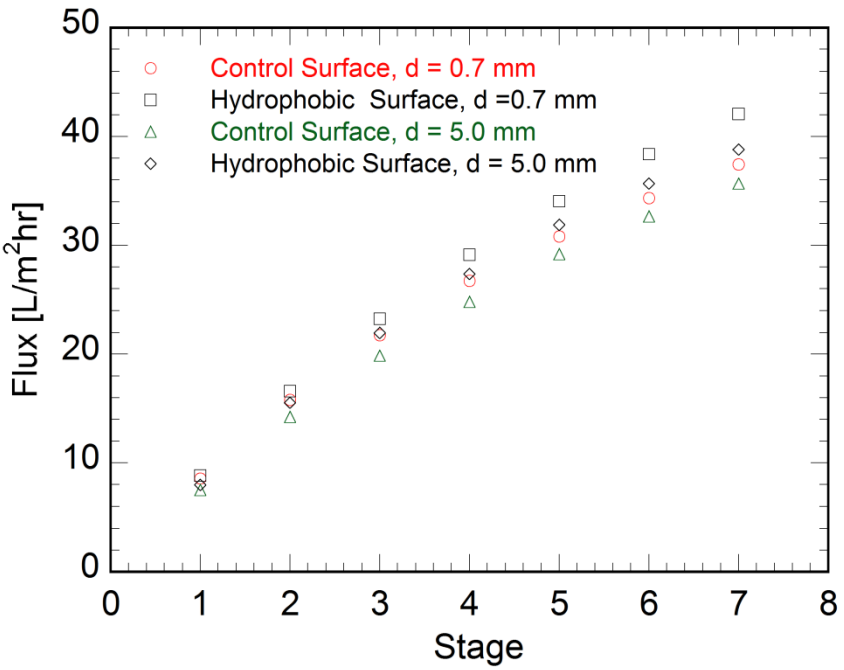

Figure 10. Cumulative Yield for the respective stages during the series configuration trials and the effect of hydrophobicity of the condensing plate and the air gap, d on the same

When this series configuration of this air-cooled system, in which the temperature of saline feed water is allowed to drop by 20 °C, is compared to single pass systems which employ a cooling channel with ΔT of 20 °C, the cumulative flux for the series configuration is about 3 times that of the single pass system in spite of the limitations of the air-cooled system. This can be seen in Figure 11.

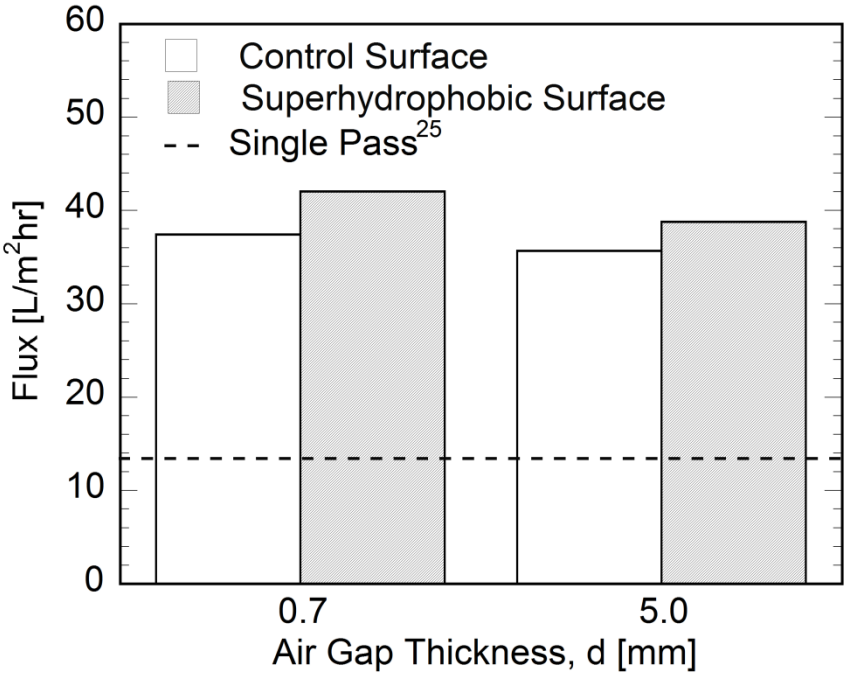

Figure 11. The overall flux obtained in series configuration with the control surface and the hydrophobic surface at different air gaps and comparison to a single pass water-cooled AGMD module with the same ΔT [25].

2.5. Conclusions

The air-cooled air gap membrane distillation system works well even though it has lower energy requirements when compared to the water-cooled system. The modular design helps us in improving the flux by adding modules in series to utilize the lower difference in temperatures of saline feed and the saline when it exits the module. The hydrophobic surface helps in improving the flux as well as reduces the temperature drop for the saline water as it passes through the module.

The conductivity of the support mesh had a significant effect on the yield from the setup. The copper mesh with its conductivity of about 401 W/m-K resulted in the highest flux values

followed by the Aluminum mesh and steel mesh. The plastic mesh resulted in about 30% lesser flux values. Hydrophobicity of the support mesh did not have as great an impact on the flux values as the conductivity values. In fact in certain cases the hydrophobic mesh resulted in lower yields when compared to the normal copper mesh.

Increasing the air gap resulted in lower flux values. The saline temperature reduced less in the case of increased air gap but the flux but it was not enough to result in an increased overall flux even in the series configuration. The hydrophobic surface works well even for the larger air gaps but the flux is lower when compared to small air gap setup.

In series configuration, the hydrophobic surface with the small air gap works best and results in about three times more yield when compared to the single pass water-cooled system.